Trend Switching Processes in Financial Markets

Tobias Preis and H. Eugene Stanley

Abstract For an intriguing variety of switching processes in nature, the underlying complex system abruptly changes at a specific point from one state to another in a highly discontinuous fashion. Financial market fluctuations are characterized by many abrupt switchings creating increasing trends ("bubble formation") and decreasing trends ("bubble collapse"), on time scales ranging from macroscopic bubbles persisting for hundreds of days to microscopic bubbles persisting only on very short time scales. Our analysis is based on a German DAX Future data base containing 13,991,275 transactions recorded with a time resolution of 10^{-2} s. For a parallel analysis, we use a data base of all S&P500 stocks providing 2,592,531 daily closing prices. We ask whether these ubiquitous switching processes have quantifiable features independent of the time horizon studied. We find striking scale-free behavior of the volatility after each switching occurs. We interpret our findings as being consistent with time-dependent collective behavior of financial market participants. We test the possible universality of our result by performing a parallel analysis of fluctuations in transaction volume and time intervals between trades. We show that these financial market switching processes have features identical to those present in phase transitions. We find that the well-known catastrophic bubbles that occur on large time scales – such as the most recent financial crisis – may not be

T. Preis
Center for Polymer Studies, Department of Physics, Boston University, 590 Commonwealth Avenue, Boston, MA 02215, USA
e-mail: mail@tobiaspreis.de
and
Institute of Physics, Johannes Gutenberg University Mainz, Staudinger Weg 7, 55128 Mainz, Germany
and
Artemis Capital Asset Management GmbH, Gartenstr. 14, 65558 Holzheim, Germany

H.E. Stanley (✉)
Center for Polymer Studies, Department of Physics, Boston University, 590 Commonwealth Avenue, Boston, MA 02215, USA
e-mail: hes@bu.edu

M. Takayasu et al. (eds.), *Econophysics Approaches to Large-Scale Business Data and Financial Crisis*, DOI 10.1007/978-4-431-53853-0_1, © Springer 2010

outliers but in fact are single dramatic representatives caused by the formation of upward and downward trends on time scales varying over nine orders of magnitude from the very large down to the very small.

1 Introduction

In physics and in other natural sciences, it is often a successful strategy to analyze the behavior of a complex system by studying the smallest components of that system. For example, the molecule is composed of atoms, the atom consists of a nucleus and electrons, the nucleus consists of protons and neutrons, and so on. The fascinating point about analyses on steadily decreasing time and length scales is that one often finds that the complex system exhibits properties which cannot only be explained by the properties of its components alone. Instead, a complex behavior can emerge due to the interactions among these components [1]. In financial markets, these components are comprised by the market participants who buy and sell assets in order to realize their trading and investment decisions. The superimposed flow of all individual orders submitted to the exchange trading system initiated by market participants and of course its change in time generate a complex system with fascinating properties, similar to physical systems.

One of the key conceptual elements in modern statistical physics is the concept of scale invariance, codified in the scaling hypothesis that functions obey certain functional equations whose solutions are power laws [2–5]. The scaling hypothesis has two categories of predictions, both of which have been remarkably well verified by a wealth of experimental data on diverse systems. The first category is a set of relations, called *scaling laws*, that serve to relate the various critical-point exponents characterizing the singular behavior of functions such as thermodynamic functions. The second category is a sort of *data collapse*, where under appropriate axis normalization, diverse data "collapse" onto a single curve called a scaling function.

Econophysics research has been addressing a key question of interest: quantifying and understanding large stock market fluctuations. Previous work was focussed on the challenge of quantifying the behavior of the probability distributions of large fluctuations of relevant variables such as returns, volumes, and the number of transactions. Sampling the far tails of such distributions require a large amount of data. However, there is a truly gargantuan amount of pre-existing precise financial market data already collected, many orders of magnitude more than for typical complex systems. Accordingly, financial markets are becoming a paradigm of complex systems, and increasing numbers of scientists are analyzing market data [6–18]. Empirical analyses have been focused on quantifying and testing the robustness of power-law distributions that characterize large movements in stock market activity. Using estimators that are designed for serially and cross-sectionally independent data, findings thus far support the hypothesis that the power law exponents that characterize fluctuations in stock price, trading volume, and the number of trades [19–26] are seemingly "universal" in the sense that they do not change their values significantly for different markets, different time periods, or different market conditions.

In contrast to these analyses of global financial market distributions we focus on the temporal sequence of fluctuations in volatility, transaction volume, and inter-trade times before and after a trend switching point. Our analysis can provide insight into switching processes in complex systems in general and financial systems in particular. The study of dramatic crash events is limited by the fortunately rare number of such events. Increasingly, one seeks to understand the current financial crisis by comparisons with the depression of the 1930s. Here we ask if the smaller financial crises – trend switching processes on all time scales – also provide information of relevance to large crises. If this is so, then the larger abundance of data on smaller crises should provide quantifiable statistical laws for *bubbles of all scales*.

2 Financial Market Data

To answer whether smaller financial crises also provide information of relevance to large crises, we perform parallel analyses of bubble formation and bursting using two different data bases on two quite different time scales: (1) from $\approx 10^1$ to $\approx 10^6$ ms, and (2) from $\approx 10^8$ to $\approx 10^{10}$ ms.

2.1 German Market: DAX Future

For the first analysis, we use a multivariate time series of the German DAX Future contract (FDAX) traded at the European Exchange (Eurex), which is one of the world's largest derivatives exchanges. A future contract is a contract to buy or sell at a specified price at a specific future date an underlying asset – in this case the German DAX index, which measures the performance of the 30 largest German companies in terms of order book volume and market capitalization.[1] The time series comprises $T_1 = 13{,}991{,}275$ transactions of three disjoint 3-month periods (see Table 1). Each end of the three disjoint periods corresponds to a last trading day of the FDAX contract which is ruled to be the third Friday of one of the quarterly months March, June, September, and December apart from the exceptions of national holidays. The data base we analyze contains the transaction prices, the volumes, and the corresponding time stamps [31–34], with a large liquidity and inter-trade times down to 10 ms, which allows us to perform an analysis of microtrends.

The time series analysis of future contracts has the advantage that the prices are created by trading decisions alone. In contrast, stock index data are derived from a weighted summation of a bunch of stock prices. Furthermore, systematic drifts

[1] More detailed information about German DAX index constituents and calculation principles can be found on http://www.deutsche-boerse.com.

Table 1 Three disjoint 3-month periods of the German DAX Future contract (FDAX) which we analyze. Additionally, the mean volume per transaction $\bar{v}$ and the mean inter-trade time $\bar{\tau}$ is given

Contract	Records	Time period	$\bar{v}$	$\bar{\tau}$ (s)
FDAX JUN 2007	3,205,353	16 March 2007 – 15 June 2007	3.628[a]	2.485[b]
FDAX SEP 2008	4,357,876	20 June 2008 – 19 September 2008	2.558[a]	1.828[b]
FDAX DEC 2008	6,428,046	19 September 2008 – 19 December 2008	2.011[a]	1.253[b]

[a] Measured in units of contract
[b] Including overnight gaps

by inflation are eliminated by construction. The theory of futures pricing based on arbitrage states that for an asset that can be stored at no cost and which does not yield any cash flows, the futures price F has to be equal to the spot price S plus the cost of financing the purchase of the underlying between the spot date and the expiry date [35, 36]. This theoretical futures price can be referred as *fair value*. In the case of the German DAX index, the underlying purchase can be financed till expiry with a loan rate. Using a continuously compounded rate r the *fair value* equation can be written as

$$F(t) = S(t)e^{rt}, \tag{1}$$

whereas t denotes the remaining time till expiry. The theoretical futures price expression – see (1) –, which simply reflects the *cost of carry*, compensates interest rate related effects of the underlying. At expiry $t = 0$, futures price and underlying price are identical.

2.2 US Market: S&P500 Stocks

For the second analysis, which focuses on macrotrends, we use price time series of daily closing prices of all stocks of the S&P500 index. This index consists of 500 large-cap common stocks which are actively traded in the United States of America.[2] The time series comprises overall $T_2 = 2{,}592{,}531$ closing prices of US stocks till 16 June 2009 which were constituent of the S&P500 at this date. Our oldest closing prices date back to 2 January 1962. The data base of closing prices we analyze contains the daily closing prices and the daily cumulative trading volume. As spot market prices undergo a significant shift by inflation over time periods of more than 40 years we study the logarithm of stock prices instead of the raw closing prices. Thus, the results between the two different data bases on two quite different time scales become more comparable.

[2] More detailed information about S&P500 constituents and calculation principles can be found on http://www.standardandpoors.com.

BookID 188016_ChapID 001_Proof# 1 - 01/02/10

3 Renormalization Method

Less studied than the large fluctuations of major national stock indices such as the S&P500 are the various jagged functions of time characterizing complex financial fluctuations down to time scales as short as a few milliseconds. These functions at first sight are not amenable to mathematical analysis because they are characterized by sudden reversals between up and down microtrends (see Figs. 1 and 2a) which can also be referred as microscopic *bubbles* on small time scales. On these small time scales evidence can be found [1[illegible]] that the three major financial market quantities of interest – price, volume, and inter-trade times – are connected in a complex way overburdening standard tools of time series analysis such as linear cross-correlation functions. Thus, more sophisticated methods are necessary in order analyze these complex financial fluctuations creating complex financial market patterns.

We do not know how to characterize the sudden microtrend reversals. For example, the time derivative of the price $p(t)$ is discontinuous. This behavior is completely different than most real world trajectories, such as a thrown ball for

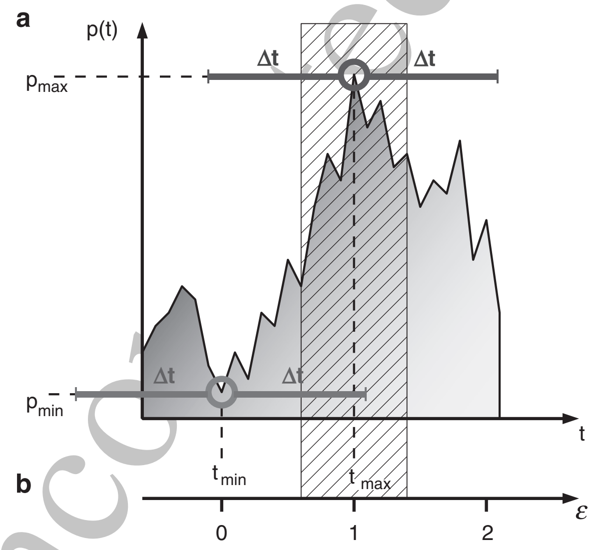

Fig. 1 Visualization of a *microtrend* in the price movement $p(t)$. (**a**) Positive microtrend starting at a local price minimum $p_{\min}$ of order Δt and ending at a local price maximum $p_{\max}$ of order Δt. The hatched region around $p_{\max}$ indicates the interval in which we find scale-free behavior of related quantities. This behavior is consistent with "self-organized" [27] macroscopic interactions among many traders [28], not unlike "tension" in a pedestrian crowd [29, 30]. The reason for tension among financial traders may be found in the risk aversions and profit targets of financial market participants. (**b**) Renormalized time scale ε between successive extrema, where $\varepsilon = 0$ corresponds to the start of a microtrend, and $\varepsilon = 1$ corresponds to the end. The hatched region is surprisingly large, starting at $\varepsilon = 0.6$ and ending at $\varepsilon = 1.4$

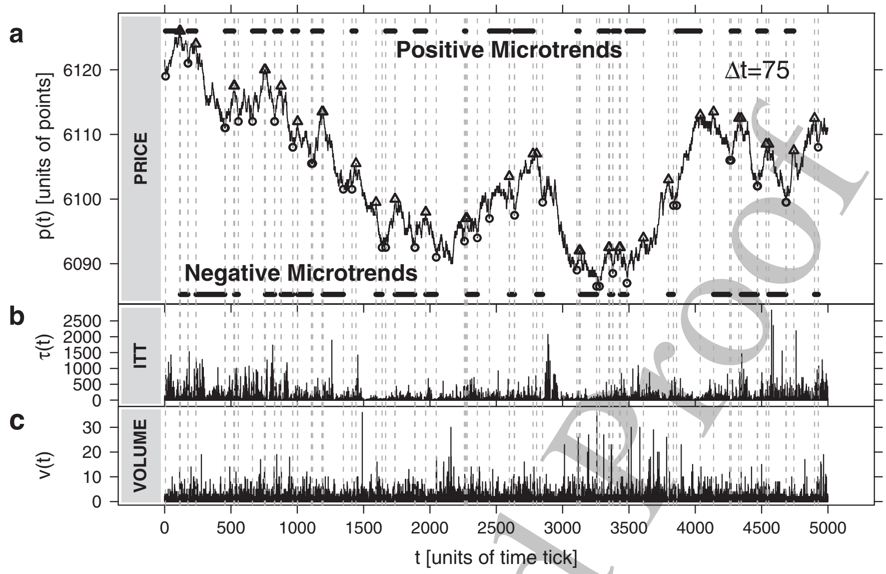

Fig. 2 Visualization of the quantities analyzed. (**a**) A small subset comprising 5,000 trades (0.04%) of the full $T_1 = 13{,}991{,}275$ trade data set analyzed, extracted from the German DAX future time series during part of one day. *Shown as circles and triangles* are the extrema of order Δt, defined to be the extremum in the interval $t - \Delta t \leq t \leq t + \Delta t$. We performed our analysis for $\Delta t = 1, 2, \ldots, 1000$ ticks; in this example, $\Delta t = 75$ ticks. Positive microtrends are indicated by *black bars on the top*, which start at a Δt-minimum and end at the next Δt-maximum. A negative microtrend (*black bars on the bottom*) starts at a Δt-maximum and ends at the consecutive Δt-minimum. (**b**) Time series of the corresponding inter-trade times $\tau(t)$ reflecting the *natural* time between consecutive trades in units of 10 ms, where $t = 1, 2, \ldots, 5000$ is the transactions index. (**c**) The volume $v(t)$ of each trade t in units of contracts

which the time derivative of the height is a smooth continuous function of time. Here we find a way of quantitatively analyzing these sudden microtrend reversals which exhibit a behavior analogous to transitions in systems in nature [2,37], and we interpret these transitions in terms of the cooperative interactions of the traders involved. A wide range of examples of transitions exhibiting scale-free behavior ranges from magnetism in statistical physics to heartbeat intervals (sudden switching from heart contraction to heart expansion) [38] and macroscopic social phenomena such as traffic flow (switching from a free traffic phase to a jammed phase) [39].

To focus on switching processes of price movements down to a microscopic time scale, we first propose how a switching process can be quantitatively analyzed. Let $p(t)$ be the transaction price of trade t, which is in the following a discrete variable $t = 1, \ldots, T$. Each transaction price $p(t)$ is defined to be a *local maximum* $p_{\max}(\Delta t)$ of order Δt if there is no higher transaction price in the interval $t - \Delta t \leq t \leq t + \Delta t$. Thus, if $p(t) = p_{\max}(t, \Delta t)$, then p(t) is a *local maximum* $p_{\max}(\Delta t)$, where

$$p_{\max}(t, \Delta t) = \max\{p(t)|t - \Delta t \leq t \leq t + \Delta t\}. \tag{2}$$

Analogously, each transaction price $p(t)$ is defined to be a *local minimum* $p_{\min}(\Delta t)$ of order Δt if there is no lower transaction price in this interval. With

$$p_{\min}(t, \Delta t) = \min\{p(t)|t - \Delta t \leq t \leq t + \Delta t\}, \tag{3}$$

it follows that $p(t)$ is a *local minimum* $p_{\min}(\Delta t)$ if $p(t) = p_{\min}(t, \Delta t)$. In this sense, the two points in the time series in Fig. 1 marked by circles are a local minimum and a local maximum, respectively. Figure 2a shows a short subset of the FDAX time series for the case $\Delta t = 7$.

For the analysis of financial market quantities in dependence of trend fraction, we introduce a renormalized time scale ε between successive extrema as follows. Let $t_{\min}$ and $t_{\max}$ be the time (measured in units of ticks) at which the corresponding transactions take place of a successive pair of $p_{\min}(\Delta t)$ and $p_{\max}(\Delta t)$ (see Fig. 1). For a positive microtrend, the renormalized time scale is given by

$$\varepsilon(t) \equiv \frac{t - t_{\min}}{t_{\max} - t_{\min}}, \tag{4}$$

with $t_{\min} \leq t \leq t_{\max} + (t_{\max} - t_{\min})$, and for a negative microtrend by

$$\varepsilon(t) \equiv \frac{t - t_{\max}}{t_{\min} - t_{\max}}, \tag{5}$$

with $t_{\max} \leq t \leq t_{\min} + (t_{\min} - t_{\max})$. Thus, $\varepsilon = 0$ corresponds to the beginning of the microtrend and $\varepsilon = 1$ indicates the end of the microtrend. We analyze a range of ε for the interval $0 \leq \varepsilon \leq 2$, so we can analyze trend switching processes both before as well as after the critical value $\varepsilon = 1$ (Fig. 1). The renormalization is essential to assure that microtrends of various lengths can be aggregated and that all switching points have a common position in the renormalized time scale.

3.1 Volatility Analysis

First we analyze the fluctuations $\sigma^2(t)$ of the price time series during the short time interval of increasing microtrends from one price minimum to the next price maximum (see Fig. 3a) and decreasing microtrends from one price maximum to the next price minimum (see Fig. 3b). The quantity studied is given by squared price differences, $\sigma^2(t) = (p(t) - p(t-1))^2$ for $t > 1$, and can be referred to as local volatility.

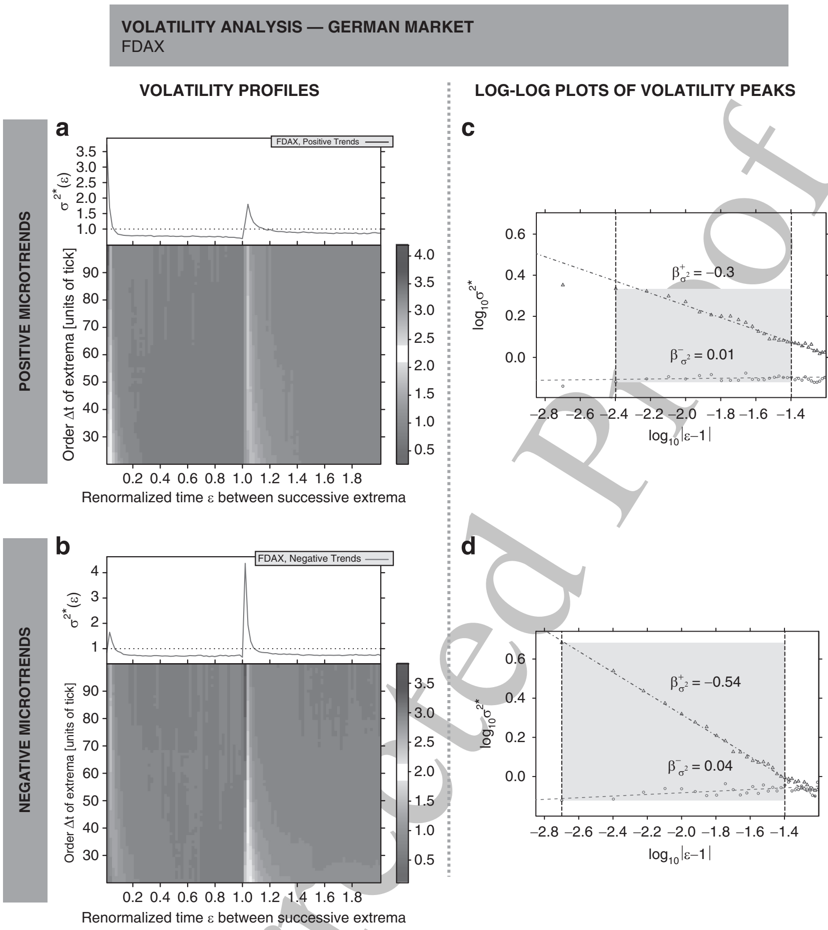

Fig. 3 Renormalization time analysis of volatility σ^2 for microtrends. (**a**) The greyscaled volatility profile, averaged over all positive microtrends in the German DAX future time series and normalized by the average volatility of all positive microtrends studied. The greyscale key gives the normalized mean volatility $\langle\sigma^2_{\text{pos}}\rangle(\varepsilon, \Delta t)/\bar{\sigma}_{\text{pos}}$. The greyscaled profile exhibits the clear link between mean volatility and price evolution. New maximum values of the price time series are reached with a significant sudden jump of the volatility, as indicated by the *vertical white regions* and the sharp maximum in the volatility aggregation $\sigma^{2*}(\varepsilon)$ shown in the *top panel*. Here, $\sigma^{2*}(\varepsilon)$ denotes the average of the volatility profile, averaged only for layers with $50 \leq \Delta t \leq 100$. After reaching new maximum values in the price the volatility decays and returns to the average value (*top panel*) for $\varepsilon > 1$. (**b**) Parallel analysis averaged over all negative microtrends in the time series. New minimum values of the price time series are reached with a pronounced sudden jump of the volatility, as indicated by the *vertical dark gray regions* in the volatility aggregation $\sigma^{2*}(\varepsilon)$ shown in the *top panel*. (**c**) The volatility (50 ticks $\leq \Delta t \leq$ 1000 ticks) before reaching a new maximum price value ($\varepsilon < 1$, *circles*) and after reaching a new maximum price value ($\varepsilon > 1$, *triangles*) aggregated for increasing microtrends. The *straight lines* correspond to power law scaling with exponents $\beta^+_{\sigma^2} = -0.30$ and $\beta^-_{\sigma^2} = 0.01$. The *shaded interval* marks the region in which this power law behavior is valid. (**d**) Log–log plot of $\sigma^{2*}(\varepsilon)$ for negative microtrends. The *straight lines* correspond to power law scaling with exponents $\beta^+_{\sigma^2} = -0.54$ and $\beta^-_{\sigma^2} = 0.04$. The *left border of the shaded region* is given by the first measuring point closest to the switching point

For the analysis of $\sigma^2(t)$ in dependence of trend direction, we use the renormalization time scale ε. In Fig. 3, the greyscale key gives the mean volatility $\langle\sigma^2\rangle(\varepsilon,\Delta t)$ in dependence of ε and Δt normalized by the average volatility $\bar{\sigma}$, where the brackets denote the average over all increasing microtrends (see Fig. 3a) or all decreasing microtrends (see Fig. 3b) in the full time series of $T_1 = 13{,}991{,}275$ records. If one can find $N_{\text{pos}}(\Delta t)$ positive microtrends and $N_{\text{neg}}(\Delta t)$ negative microtrends, each of order Δt in the time series and $\sigma_i^2(\varepsilon)$ denotes the local volatility at position ε in the i-th positive or i-th negative microtrend, then the mean volatility is given by

$$\langle\sigma^2_{\text{pos}}\rangle(\varepsilon,\Delta t) = \frac{1}{N_{\text{pos}}(\Delta t)} \sum_{i=1}^{N_{\text{pos}}(\Delta t)} \sigma_i^2(\varepsilon) \tag{6}$$

for positive microtrends and

$$\langle\sigma^2_{\text{neg}}\rangle(\varepsilon,\Delta t) = \frac{1}{N_{\text{neg}}(\Delta t)} \sum_{i=1}^{N_{\text{neg}}(\Delta t)} \sigma_i^2(\varepsilon) \tag{7}$$

for negative microtrends. The mean volatility can be normalized by the average volatility $\bar{\sigma}$ which is determined by

$$\bar{\sigma}_{\text{pos}} = \frac{\varepsilon_{\text{bin}}}{\varepsilon_{\max}\Delta t_{\max}} \sum_{\varepsilon=0}^{\varepsilon_{\max}/\varepsilon_{\text{bin}}} \left(\sum_{\Delta t=0}^{\Delta t_{\max}} \langle\sigma^2_{\text{pos}}\rangle(\varepsilon,\Delta t) \right) \tag{8}$$

and

$$\bar{\sigma}_{\text{neg}} = \frac{\varepsilon_{\text{bin}}}{\varepsilon_{\max}\Delta t_{\max}} \sum_{\varepsilon=0}^{\varepsilon_{\max}/\varepsilon_{\text{bin}}} \left(\sum_{\Delta t=0}^{\Delta t_{\max}} \langle\sigma^2_{\text{neg}}\rangle(\varepsilon,\Delta t) \right), \tag{9}$$

whereas $\varepsilon_{\max}$ is the maximum value of the renormalization time scale ε studied, which is fixed to $\varepsilon_{\max} = 2$ and ε_{bin} denotes the bin size of the renormalization time scale. The maximum value of the extrema order Δt which we analyze is given by $\Delta t_{\max}$. The bin size is related to $\Delta t_{\max}$ by

$$\varepsilon_{\text{bin}} = \frac{\varepsilon_{\max}}{\Delta t_{\max}} \tag{10}$$

for convenience reasons. The absence of changes of the greyscaled volatility profiles in Fig. 3 is consistent with a *data collapse* for Δt values larger than a certain cut-off value Δt_{cut}. Thus, we calculate the volatility aggregation $\sigma^{2*}(\varepsilon)$. This volatility aggregation $\sigma^{2*}(\varepsilon)$ is the average of the mean volatility $\langle\sigma^2_{\text{neg}}\rangle(\varepsilon,\Delta t)$, averaged only for layers with $\Delta t_{\text{cut}} \le \Delta t \le \Delta t_{\max}$. It is given by

$$\sigma^{2*}_{\text{pos}}(\varepsilon) = \frac{1}{\Delta t_{\max} - \Delta t_{\text{cut}}} \sum_{\Delta t=\Delta t_{\text{cut}}}^{\Delta t_{\max}} \frac{\langle\sigma^2_{\text{pos}}\rangle(\varepsilon,\Delta t)}{\bar{\sigma}_{\text{pos}}} \tag{11}$$

and the equivalent definition

$$\sigma^{2*}_{\mathrm{neg}}(\varepsilon) = \frac{1}{\Delta t_{\max} - \Delta t_{\mathrm{cut}}} \sum_{\Delta t = \Delta t_{\mathrm{cut}}}^{\Delta t_{\max}} \frac{\langle \sigma^2_{\mathrm{neg}} \rangle (\varepsilon, \Delta t)}{\bar{\sigma}_{\mathrm{neg}}} \tag{12}$$

for negative microtrends. Note that in order to improve the readability the subscripts "pos" and "neg" are removed if the context assures whether positive or negative microtrends are considered.

The greyscaled volatility profiles (see Fig. 3) provide the mean volatility $\langle \sigma^2 \rangle (\varepsilon, \Delta t)$ averaged over all increasing or all decreasing microtrends in the full time series of $T_1 = 13{,}991{,}275$ records, and are normalized by the average volatilities of microtrends studied in both cases. In order to remove outliers, only those microtrends are collected in which the time intervals between successive trades $\tau(t)$ [40] (Fig. 2b) are not longer than 1 min, which is roughly 60 times longer than the average inter-trade time (≈0.94 s without overnight gaps), and in which the transaction volumes are not larger than 100 contracts (the average transaction volume is 2.55 contracts, see Table 1). This condition ensures that time which is measured in units of ticks runs only over the working hours of the exchange – removing overnight gaps, weekends, and national holidays. Furthermore, the analysis is only based on those microtrends which provide a reasonable activity. The greyscale profiles exhibit a very clear link between volatility and price evolution. A new local price maximum is reached with a significant sudden jump of the volatility (top panel of Fig. 3a). After reaching new local maximum values in the price the volatility decays and returns to the average value for $\varepsilon > 1$. The reaching of a maximum causes obviously tension among the market participants. A local price maximum can stir the expectations that higher prices are possible and thus animate for purchases. This development can also raise fears of traders to find an optimal price for selling their assets. Additionally, it is possible that market participants holding a short position which means that they benefit from falling asset prices have to cut their losses by reaching new maximum values. For negative microtrends, the reaching of local minimum values in the price coincides with a more pronounced sudden jump of the volatility (see Fig. 3b). A negative asset price evolution seems to create a situation in which market participants act in a more dramatic way after the end of a trend in comparison to the end of positive microtrends. One can conjecture that they are driven by tension at least or even by "panic" if they try to cut their losses. But of course, also the opposite situation should become relevant: A market participant who has no inventory is looking for entry opportunities. As asset prices are rising after reaching a local price minimum ($\varepsilon = 1$), a financial market actor, who has the intention to enter into the market, has to deal with the tension to find the "right" time – the optimal entry level is already missed at this time: the local price minimum.

This qualitative effect is intuitively understandable and should be obvious for market actors. In contrast, the shape of the volatility peak around extrema is surprising. The peak is characterized by asymmetric tails, which we analyze next. For this analysis, we use the volatility aggregation $\sigma^{2*}(\varepsilon)$, which is the mean volatility

$\langle\sigma^2\rangle(\varepsilon, \Delta t)$ averaged for layers from $\Delta t_{\text{cut}} = 50$ ticks to $\Delta t_{\max} = 1000$ ticks. Figure 3c shows the aggregated average volatility $\sigma^{2*}(\varepsilon)$ for positive microtrends on a log–log plot. Surprisingly, the evolution of the volatility before and after reaching a maximum shows up as straight lines and thus are consistent with a power law scaling behavior

$$\sigma^{2*}(|\varepsilon - 1|) \sim |\varepsilon - 1|^{\beta_{\sigma^2}} \tag{13}$$

within the range indicated by the vertical dashed lines. Over one order of magnitude, we find distinct exponents, $\beta^-_{\sigma^2} = 0.01$ before a price maximum and $\beta^+_{\sigma^2} = -0.30$ after. Figure 3d shows the aggregated average volatility $\sigma^{2*}(\varepsilon)$ for negative microtrends on a log–log plot. Over more than one order of magnitude, we find for negative microtrends a qualitatively consistent behavior to positive microtrends with distinct exponents, $\beta^-_{\sigma^2} = 0.04$ before a price minimum and $\beta^+_{\sigma^2} = -0.54$ after.

Next we test the possible universality of our results by performing a parallel analysis for trends on long time scales using the daily closing price data base of S&P500 stocks. In this sense universality means that our renormalized market quantities do not change their values significantly for different markets, different time periods, or different market conditions.

Note that for our parallel analysis on macroscopic time scales the order of a extremum Δt is measured in units of days, and that $\langle\sigma^2\rangle(\varepsilon, \Delta t)$ is averaged additionally over all closing price time series of all S&P500 components. In order to avoid biased contributions for the rescaled averaging caused by inflation based drifts over more than 47 years as described in Sect. 2.2, the analyzed price time series $p(t)$ contains the logarithm of the daily closing prices. Figure 4a shows the mean volatility $\langle\sigma^2\rangle(\varepsilon, \Delta t)$ for positive microtrends averaged for layers from $\Delta t_{\text{cut}} = 10$ days to $\Delta t_{\max} = 100$ days. Figure 4b shows the mean volatility $\langle\sigma^2\rangle(\varepsilon, \Delta t)$ for negative microtrends averaged for the same layers' range. As already uncovered for microtrends, the sudden volatility rise is more dramatic for negative macrotrends than for positive macrotrends. The aggregated average volatilities $\sigma^{2*}(\varepsilon)$ for positive and negative macrotrends on a log–log plot show surprisingly again distinct tail exponents around the switching point $\varepsilon = 1$. For positive macrotrends, we obtain $\beta^-_{\sigma^2} = -0.05$ before a price maximum and $\beta^+_{\sigma^2} = -0.40$ after. For negative microtrends, we obtain $\beta^-_{\sigma^2} = -0.09$ before a price minimum and $\beta^+_{\sigma^2} = -0.50$ after, which is both similar to the values obtained for our study of positive and negative microtrends.

3.2 Volume Analysis

To test the possible universality of these results obtained for volatility, we perform a parallel analysis of the corresponding volume fluctuations $v(t)$, the numbers of contracts traded in each individual transaction (see Fig. 2c) in case of microtrends for the German market and the cumulative number of traded stocks per day in case of macrotrends for the US market. In Fig. 5a, the greyscaled volume profile provides the mean volume averaged over all increasing microtrends in the time series of the

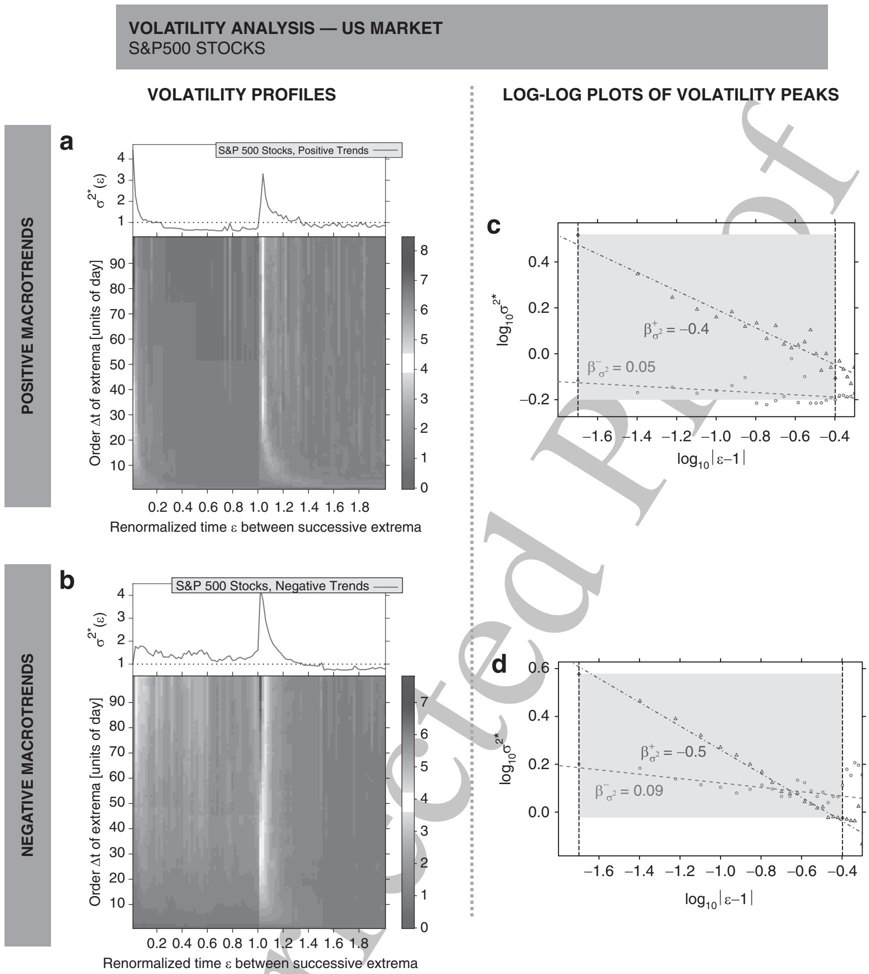

Fig. 4 Renormalization time analysis of volatility σ^2 for macrotrends. (**a**) The greyscaled volatility profile, averaged over all positive macrotrends in the daily closing price time series of all S&P500 stocks and normalized by the average volatility of all positive macrotrends studied. The stylized fact that new maximum values of the price time series are reached with a significant sudden jump of the volatility can also be found for macrotrends. Note that Δt is measured in units of day for macrotrends. (**b**) Parallel analysis performed for all negative macrotrends in the daily closing price time series of all S&P500 stocks. As already uncovered for microtrends (see Fig. 3), the sudden jump of the volatility at $\varepsilon = 1$ is more pronounced for negative trends than for positive microtrends. (**c**) The volatility (10 days $\leq \Delta t \leq$ 100 days) before reaching a new maximum price value ($\varepsilon < 1$, *circles*) and after reaching a new maximum price value ($\varepsilon > 1$, *triangles*) aggregated for increasing macrotrends. The *straight lines* correspond to power law scaling with exponents $\beta^+_{\sigma^2} = -0.40$ and $\beta^-_{\sigma^2} = -0.05$. (**d**) Log–log plot of $\sigma^{2*}(\varepsilon)$ for negative macrotrends. The *straight lines* correspond to power law scaling with exponents $\beta^+_{\sigma^2} = -0.50$ and $\beta^-_{\sigma^2} = -0.09$

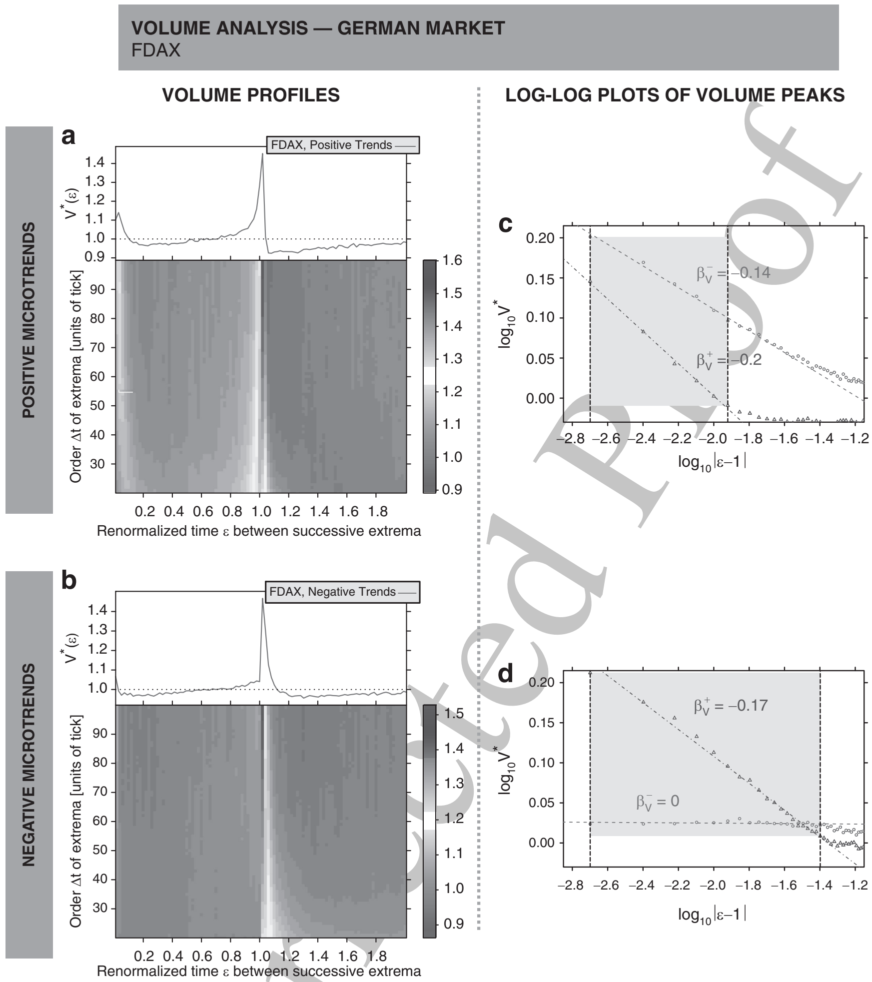

Fig. 5 Renormalization time analysis of volume for microtrends. (**a**) The greyscaled volume profile, averaged over all positive microtrends in the FDAX time series and normalized by the average volume of all positive microtrends studied. New maximum values of the price time series coincide with peaks in the volume. (**b**) Parallel analysis performed for all negative microtrends in FDAX time series. (**c**) The volume (50 ticks $\leq \Delta t \leq$ 1000 ticks) before reaching a new maximum price value ($\varepsilon < 1$, *circles*) and after reaching a new maximum price value ($\varepsilon > 1$, *triangles*) aggregated for increasing microtrends. The *straight lines* correspond to power law scaling with exponents $\beta_v^+ = -0.20$ and $\beta_v^- = -0.14$. (**d**) Log–log plot of $v^*(\varepsilon)$ for negative microtrends. The *straight lines* correspond to power law scaling with exponents $\beta_v^+ = -0.17$ and $\beta_v^- = 0$

German market and is also normalized by the average volume of all microtrends studied. Analogously, Fig. 5b shows the mean volume averaged over all decreasing microtrends in the time series. In order to remove outliers in this analysis, we consider only those microtrends which include inter-trade times not longer than

1 min and transaction volumes not larger than 100 contracts. As expected, new price extrema are linked with peaks in the volume time series but, surprisingly, we find that the usual cross-correlation function between price changes and volumes vanishes. Thus, one can conjecture that the tendency to increased volumes occurring at the end of positive microtrends is counteracted by the tendency to increased volumes occurring at the end of negative microtrends. The crucial issue is to distinguish between positive and negative microtrends realized by the renormalization time ε between successive extrema.

For positive microtrends, a significant increase of volumes can be found already before the local maximum price is reached. After reaching the local maximum value the volatility falls dramatically back to values close to the average value. For negative microtrends, the opposite characteristic is observable. The reaching of a local price minimum causes a sudden jump of the transaction volume, whereas after the local price minimum the volume decays and returns to the average value for $\varepsilon > 1$. In the top panel of Figs. 5a,b, we show the volume aggregations $v^*(\varepsilon)$, obtained by averaging Δt "slices" between $\Delta t_{\mathrm{cut}} = 50$ and $\Delta t_{\max} = 100$. Figure 5c shows $v^*(\varepsilon)$ versus $|\varepsilon - 1|$ as a log–log histogram supporting a power law behavior of the form

$$v^*(|\varepsilon - 1|) \sim |\varepsilon - 1|^{\beta_v} \tag{14}$$

with exponents $\beta_v^- = -0.14$ before, and $\beta_v^+ = -0.20$ after a price maximum – $v^*(\varepsilon)$ is obtained by averaging Δt "slices" between $\Delta t_{\mathrm{cut}} = 50$ and $\Delta t_{\max} = 1000$. For negative microtrends, straight lines can be detected in the log–log histogram as well with exponents $\beta_v^- = -0.17$ before, and $\beta_v^+ = 0$ after a local price minimum (Fig. 5d).

A parallel analysis for the US market on large time scales (Figs. 6a,b) provides evidence that the volume peaks are symmetrically shaped around the switching point $\varepsilon = 1$ and that the characteristics are similar for positive and negative macrotrends. The power law exponents for positive microtrends are given by $\beta_v^- = -0.04$ before, and $\beta_v^+ = -0.08$ after a local price maximum (Fig. 6c). The similar behavior of negative microtrends is supported by exponents $\beta_v^- = -0.05$ before, and $\beta_v^+ = -0.15$ after a local price minimum as shown in Fig. 6d.

3.3 Inter-trade Time Analysis

In order to verify a possible universality, we analyze additionally the behavior of the inter-trade times $\tau(t)$ of the German market during the short time interval from one price extremum to the next (see Fig. 2b). The linear cross-correlation function between price changes and inter-trade times as standard tool of time series analysis exhibits no significant correlation values as well. Thus, one can again conjecture that the tendency to decreased inter-trade times for the end of positive microtrends is counteracted by the tendency to decreased inter-trade times for the end of negative microtrends. It is of crucial importance to distinguish between positive and negative

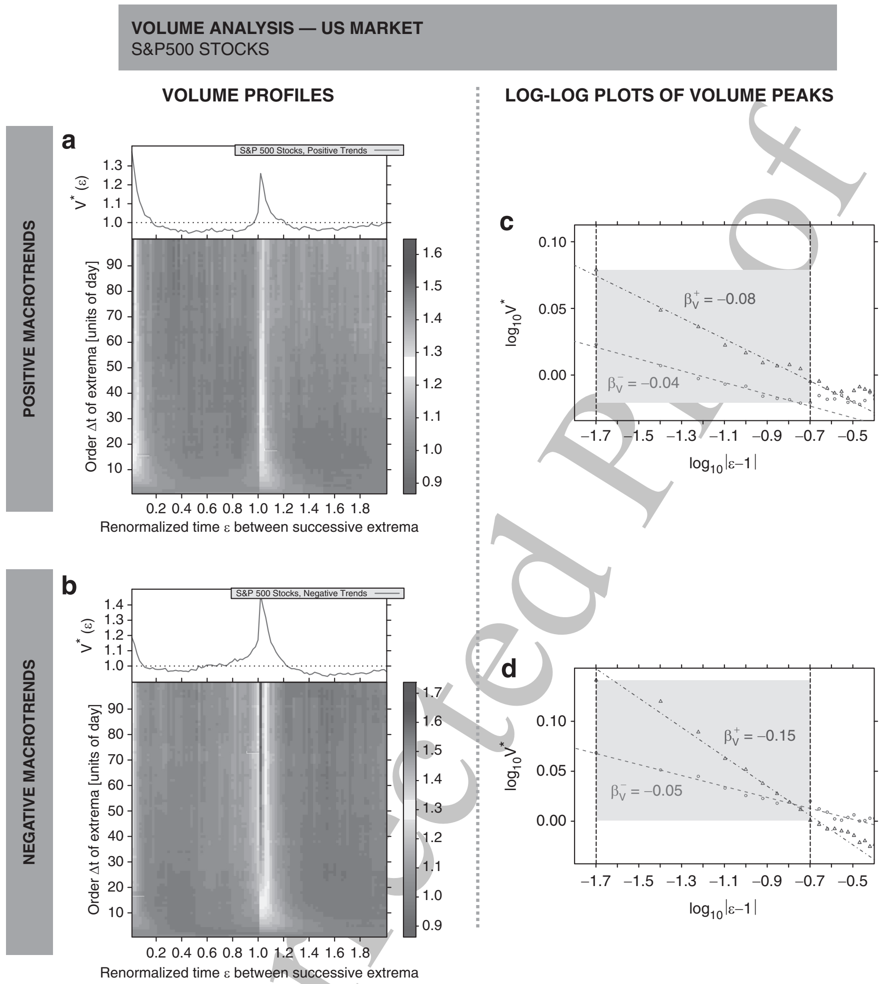

Fig. 6 Renormalization time analysis of volume for macrotrends. (**a**) The greyscaled volume profile, averaged over all positive macrotrends in the daily closing price time series of all S&P500 stocks and normalized by the average volatility of all positive macrotrends studied. Consistent with our results for microtrends maximum values of the price time series are reached with a peak of the volume. Note that Δt is measured in units of day for macrotrends. (**b**) Parallel analysis performed for all negative macrotrends in the daily closing price time series of all S&P500 stocks. Minimum values of the price time series coincide with peaks of volume as for positive macrotrends. (**c**) The volume (10 days $\leq \Delta t \leq$ 100 days) before reaching a new maximum price value ($\varepsilon < 1$, *circles*) and after reaching a new maximum price value ($\varepsilon > 1$, *triangles*) aggregated for increasing macrotrends. The straight lines correspond to power law scaling with exponents $\beta_v^+ = -0.08$ and $\beta_v^- = -0.04$. (**d**) Log–log plot of $v^*(\varepsilon)$ for negative macrotrends. The *straight lines* correspond to power law scaling with exponents $\beta_v^+ = -0.15$ and $\beta_v^- = -0.05$

microtrends realized by the renormalized time ε between successive extrema. In Figs. 7a and 7b, the mean inter-trade time $\langle\tau\rangle(\varepsilon, \Delta t)/\bar{\tau}$ is shown for positive and negative microtrends, respectively, mirroring the clear link between inter-trade times and price extrema. Far away from the critical point $\varepsilon = 1$ the mean inter-trade time starts to decrease. After the formation of a new local price maximum the mean inter-trade times increase and return to the average value in a very symmetrical way. Negative microtrends obey the same behavior with one exception. The reaching of a local price minimum ($\varepsilon = 1$) coincides with a temporary sudden increase of the inter-trade times. For both types of trends, the dip of the inter-trade times can be interpreted in terms of "panic". Close before reaching local price extreme values market participants try to participate in the forming trend or try to correct their trading decision which was caused by the hope to participate in an opposite trend formation. After reaching the local price extreme value, the tension persists but becomes steadily smaller.

In the top panels of Figs. 7a,b, the aggregation of the inter-trade time profile $\tau^*(\varepsilon)$ is shown calculated for all values of Δt between $\Delta t_{\mathrm{cut}} = 50$ and $\Delta t_{\max} = 100$. Figure 7c shows $\tau^*(\varepsilon)$ versus $|\varepsilon - 1|$ as a log–log histogram supporting a power law behavior of the form

$$\tau^*(|\varepsilon - 1|) \sim |\varepsilon - 1|^{\beta_\tau} \qquad (15)$$

for positive microtrends with exponents $\beta_\tau^- = 0.10$ before, and $\beta_\tau^+ = 0.12$ after a local price maximum. For negative microtrends, we obtain exponents $\beta_\tau^- = 0.09$ before, and $\beta_\tau^+ = 0.15$ after a local price minimum (see Fig. 7d). A log–log histogram of a parallel analysis for the US market on large time scales is not obtainable as the inter-trade times between successive closing prices are given by the constant value of 1 day (exceptions are weekends and general holidays).

3.4 Random Shuffling

To confirm that our results are a consequence of the exact time series sequence and thus sensitive to the time ordering of the original time series of volumes and inter-trade times, we randomly shuffle γT pairs of data points of both the volume time series and inter-trade time series in order to weaken their connection with the price evolution. We find that the clear link between volumes fluctuations and price evolution (see Fig. 8a) and between inter-trade times and price evolution (see Fig. 8b) disappears with increasing γ and entirely vanishes for $\gamma \geq 1$ for microtrends. The dip of the inter-trade times at $\varepsilon = 1$ becomes less pronounced with increasing γ and, correspondingly, the peak of the volume maximum decreases. For the S&P500 data set (Fig. 8c), the volume peak disappears with increasing γ obeying the same characteristics. These shuffling induced processes can also be characterized by power law relationships which support our result that a fluctuating price time series passes through a sequence of distinct transitions with scale-free properties. The disappearance phenomenon follows a power law behavior. The maximum value of $v^*(\varepsilon)_\gamma$ at $\varepsilon = 1$ scales with exponent $\beta_v^s = -0.12$ for microtrends (Fig. 8d). The

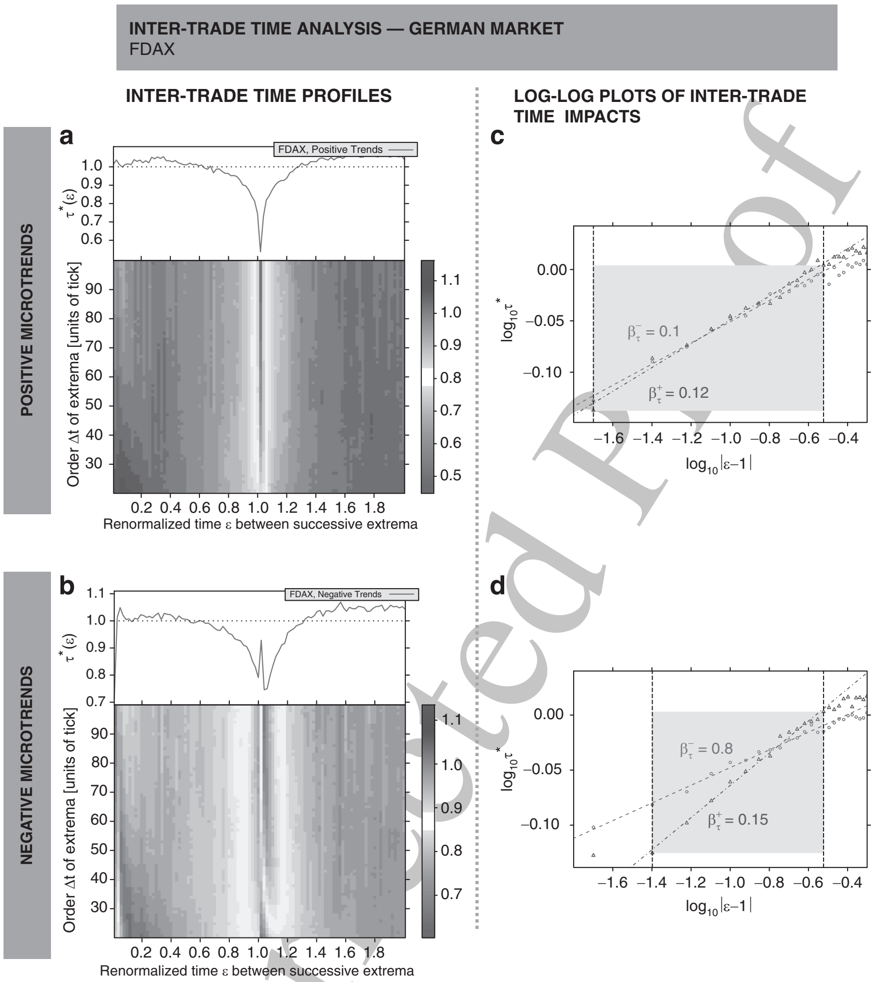

Fig. 7 Renormalization time analysis of inter-trade times for microtrends. (**a**) The greyscaled inter-trade time profile – averaged over all increasing microtrends in the German DAX Future time series and normalized by the average inter-trade times of all positive microtrends studied – is performed analogously to our study of volatility and volume. New maximum values of the price time series are reached with a significant decay of the inter-trade times. (**b**) Parallel analysis performed for all negative microtrends in the FDAX price time series. Minimum values of the price time series coincide with a dip of inter-trade times. In contrast to increasing trends, we observe for exactly $\varepsilon = 1$ an interim increase of the inter-trade times. (**c**) Inter-trade times (50 ticks $\leq \Delta t \leq$ 100 ticks) before reaching a new maximum price value ($\varepsilon < 1$, *circles*) and after reaching a new maximum price value ($\varepsilon > 1$, *triangles*) aggregated for increasing microtrends. The *straight lines* correspond to power law scaling with exponents $\beta_\tau^+ = 0.12$ and $\beta_\tau^- = 0.10$. (**d**) Log–log plot of $\tau^*(\varepsilon)$ for negative microtrends. The *straight lines* correspond to power law scaling with exponents $\beta_\tau^+ = 0.15$ and $\beta_\tau^- = 0.08$

BookID 188016_ChapID 001_Proof# 1 - 01/02/10

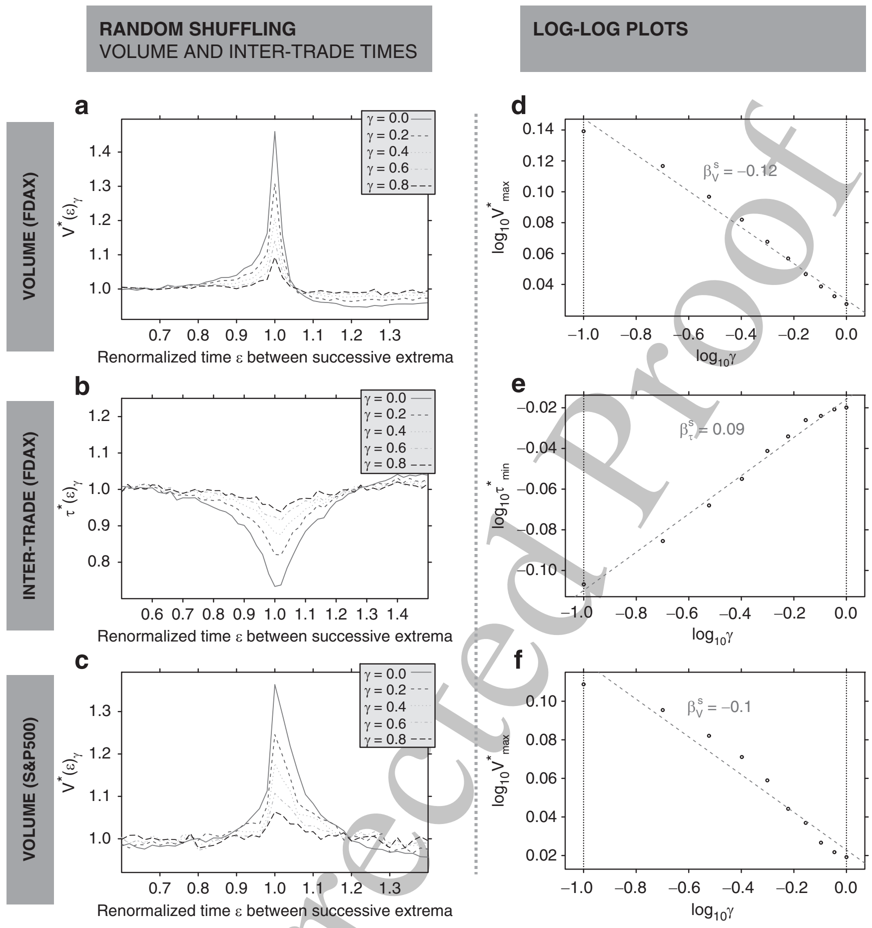

Fig. 8 Stability test of power law dependency. (**a**) If one shuffles randomly γT pairs of volume entries in the multivariate time series, the significant link between volume and price evolution starts to disappear as γ increases. (**b**) If γT pairs of inter-trade time entries are randomly shuffled the inter-trade time dip starts to disappear. (**c**) We find an identical behavior for the volume peak on long time scales using daily closing prices of S&P500 stocks. (**d**) The disappearance phenomenon also follows a power law behavior. The maximum value of $v^*(\varepsilon)_\gamma$ at $\varepsilon = 1$ scales with exponent $\beta^s_v = -0.115 \pm 0.005$. (**e**) The minimum value of $\tau^*(\varepsilon)_\gamma$ at $\varepsilon = 1$ scales with exponent $\beta^s_v = 0.094 \pm 0.004$. (**f**) In the case of the maximum of $v^*(\varepsilon)_\gamma$ at $\varepsilon = 1$ for the S&P500 stocks, the plot provides a power law with exponent $\beta^s_v = -0.095 \pm 0.008$

minimum value of $\tau^*(\varepsilon)_\gamma$ at $\varepsilon = 1$ scales with exponent $\beta^s_v = 0.09$ as shown in Fig. 8e. In the case of the maximum of $v^*(\varepsilon)_\gamma$ at $\varepsilon = 1$ on large time scales, the log–log plot provides a straight line with a power law exponent $\beta^s_v = -0.10$ for the S&P500 stocks which is consistent with the underlying data set. In fact, deviations can be observed for macrotrends which are caused by the limited number of closing prices in the S&P500 data base ($T_2 \ll T_1$).

3.5 Universality of Power Law Exponents

Thus far, we distinguished between positive and negative trends on small and large time scales. In order to emphasize the possible universality of our results we present in this section a direct comparison of microtrends and macrotrends for our three financial market quantities of interest – volatility, volume, and inter-trade times. Figure 9 shows the renormalization time analysis of volatility σ^2, trade volumes v, and inter-trade times τ for all increasing and decreasing microtrends in the German DAX Future time series. The greyscaled volatility profile exhibits the clear link between mean volatility and price evolution. New extreme values of the price time series are reached with a significant sudden jump of the volatility, as indicated by the vertical dark gray regions and the sharp maximum in the volatility aggregation. After reaching new extreme values in the price, the volatility decays and returns to the average value for $\varepsilon > 1$ as observed in Sect. 3.1 for positive and negative microtrends, respectively. The greyscaled volume profile exhibits that the volume is clearly connected to the price evolution: new extreme values of the price coincide

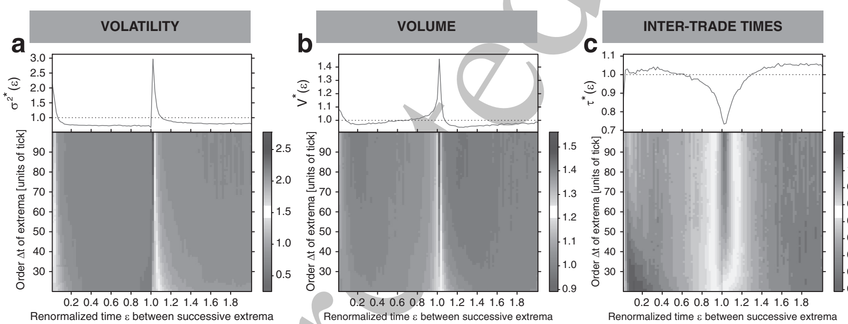

Fig. 9 Renormalization time analysis of volatility σ^2, trade volumes v, and inter-trade times τ for all microtrends – increasing and decreasing microtrends. (**a**) The greyscaled volatility profile, averaged over all microtrends in the time series and normalized by the average volatility of all microtrends studied. We analyze both positive and negative microtrends. The greyscale code gives the normalized mean volatility $\langle\sigma^2\rangle(\varepsilon, \Delta t)/\bar{\sigma^2}$. The greyscaled profile exhibits the clear link between mean volatility and price evolution. New extreme values of the price time series are reached with a significant sudden jump of the volatility, as indicated by the *vertical dark gray regions* and the sharp maximum in the volatility aggregation $\sigma^{2*}(\varepsilon)$ shown in the *top panel*. Here, $\sigma^{2*}(\varepsilon)$ denotes the average of the volatility profile, averaged only for layers with $50 \leq \Delta t \leq 100$. After reaching new extreme values in the price the volatility decays and returns to the average value (*top panel*) for $\varepsilon > 1$. (**b**) The greyscaled volume profile, averaged over all microtrends in the time series and normalized by the average volume of all microtrends studied. The greyscale code gives the normalized mean volume $\langle v\rangle(\varepsilon, \Delta t)/\bar{v}$. The volume is connected to the price evolution: new extreme values of the price coincide with peaks in the volume time series, as indicated by the *vertical dark gray regions* close to $\varepsilon = 1$. The *top panel* shows the volume aggregation $v^*(\varepsilon)$, where $v^*(\varepsilon)$ is the average over layers with $50 \leq \Delta t \leq 100$. The sharp maximum in $v^*(\varepsilon)$ is shown in the *top panel*. (**c**) The greyscaled inter-trade time profile – averaged over all microtrends in the time series and normalized by the average inter-trade times of all microtrends studied – is performed analogously to our study of volatility and volume. New extreme values of the price time series are reached with a significant decay of the inter-trade times

with peaks in the volume time series, as indicated by the vertical dark gray regions 353
close to $\varepsilon = 1$. The greyscaled inter-trade time profile shows that new extreme 354
values of the price time series are reached with a significant decay of the inter-trade 355
times. The log–log plots of all these quantities can be found in Fig. 10. Additionally, 356
the time scales which we study are visualized for both the German market and the 357
US market. For the analysis of microtrends, we use the German DAX future data 358
base which enables us to analyze microtrends starting at roughly 10^6 ms down to 359

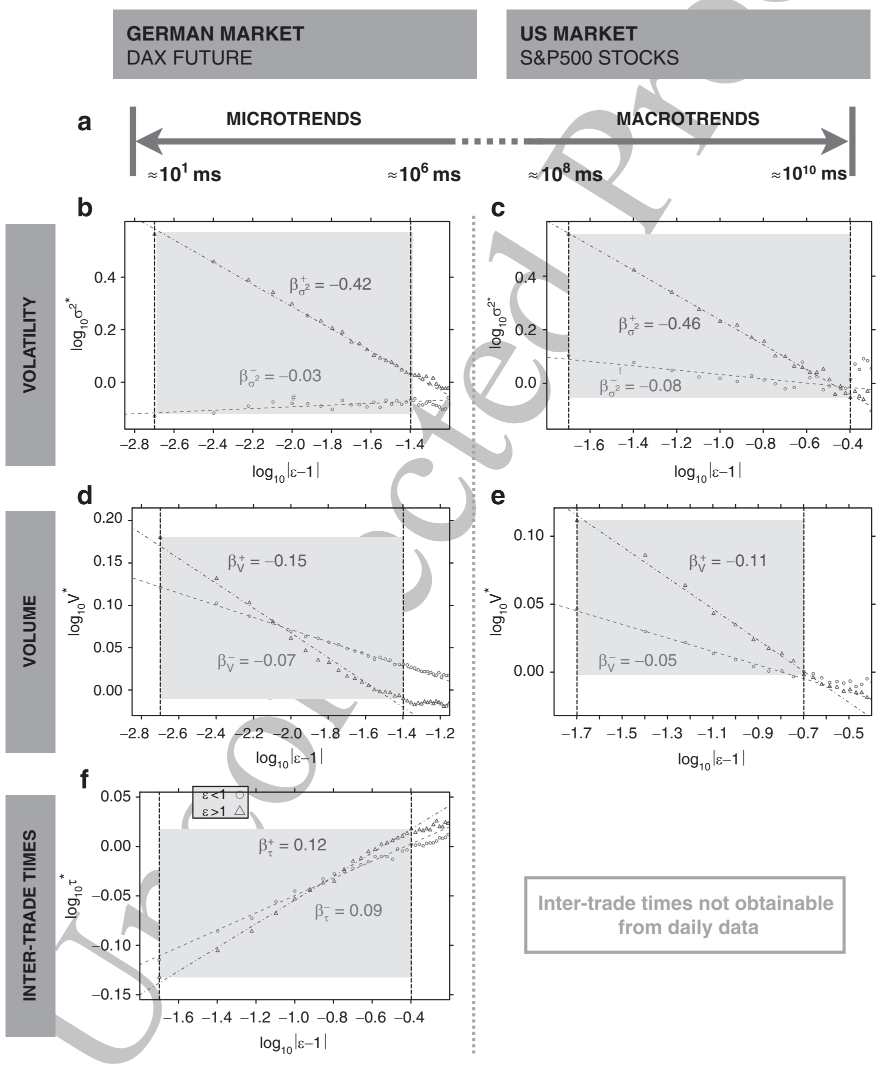

Fig. 10 Overview of time scales studied and log–log plots of quantities with scale-free properties. (**a**) Visualization of time scales studied for both the German market and the US market. For the analysis of microtrends, we use the German DAX future data base which enables us to analyze

BookID 188016_ChapID 001_Proof# 1 - 01/02/10

the smallest possible time scale of individual transactions measured in multiples of 10 ms. The log–log plots of quantities with scale-free behavior on short time scales are shown in the left column. For the analysis of macrotrends, we use the data base of daily closing prices of all S&P500 stocks which enables us to perform an equivalent analysis of macrotrends on long time scales which are shown the right column. Thus, our analysis of switching processes ranges over nine orders of magnitude from 10 to 10^{10} ms. Surprisingly, the region around an extreme value in which the power law scaling can be found is large, especially for inter-trade waiting times on small time scales (see Fig. 10f) and volumes on long time scales (see Fig. 10c). This range around a local extreme price value is marked as hatched region in Fig. 1. Far away from the switching point a tension among market participants is established and propagates steadily until the critical point is reached – the switching point changing from an upward to a downward or from a downward to an upward trend.

4 Summary and Conclusions

The straight lines in Fig. 10 offer insight into financial market fluctuations: (1) a clear connection between volatility, volumes, inter-trade times, and price fluctuations on the path from one extremum to the next extremum, and (2) the underlying law, which describes the tails of volatility, volumes, and inter-trade times around extrema varying over nine orders of magnitude starting from the smallest possible time

Fig. 10 (continued) microtrends starting at roughly 10^6 ms down to the smallest possible time scale of individual transactions measured in multiples of 10 ms. The log–log plots of quantities with scale-free behavior on short time scales are shown in the left column. For the analysis of macrotrends, we use the data base of daily closing prices of all S&P500 stocks which enables us to perform equivalent analysis of macrotrends on long time scales which are shown the *right column*. Thus, our analysis of switching processes ranges over nine orders of magnitude from 10 to 10^{10} ms. (**b**) The volatility (50 ticks $\leq \Delta t \leq$ 1000 ticks) before reaching a new extreme price value ($\varepsilon < 1$, *circles*) and after reaching a new extreme price value ($\varepsilon > 1$, *triangles*) aggregated for microtrends. The *straight lines* correspond to power law scaling with exponents $\beta^{+}_{\sigma^2} = -0.42 \pm 0.01$ and $\beta^{-}_{\sigma^2} = 0.03 \pm 0.01$. The *shaded interval* marks the region in which this power law behavior is valid. The *left border of the shaded region* is given by the first measuring point closest to the switching point. (**c**) The volatility aggregation of macrotrends determined for the US market on long time scales (10 days $\leq \Delta t \leq$ 100 days). The *straight lines* correspond to power law scaling with exponents $\beta^{+}_{\sigma^2} = -0.46 \pm 0.01$ and $\beta^{-}_{\sigma^2} = -0.08 \pm 0.02$ which are consistent with the exponents determined for the German market on short time scales. (**d**) Log–log plot of the volume aggregation on short time scales (50 ticks $\leq \Delta t \leq$ 1000 ticks) exhibits a power law behavior with exponents $\beta^{+}_{v} = -0.146 \pm 0.005$ and $\beta^{-}_{v} = -0.072 \pm 0.001$. (**e**) Log–log plot of the volume aggregation on long time scales (10 days $\leq \Delta t \leq$ 100 days) exhibits a power law behavior with exponents $\beta^{+}_{v} = -0.115 \pm 0.003$ and $\beta^{-}_{v} = -0.050 \pm 0.002$ which are consistent with our results for short time scales. (**f**) Log–log plot of the inter-trade time aggregation on short time scales (50 ticks $\leq \Delta t \leq$ 100 ticks) exhibits a power law behavior with exponents $\beta^{+}_{\tau} = 0.120 \pm 0.002$ and $\beta^{-}_{\tau} = 0.087 \pm 0.002$. An equivalent analysis on long time scales is not possible as daily closing prices are recorded with equidistant time steps scale, is a power law with a unique exponents which quantitatively characterize the region around the trend switching point. As a direct consequence of the existence of power law tails, the behavior does not depend on the scale. Thus, we find identical behavior for other sub-intervals of $50 \leq \Delta t \leq 1000$. With a decreasing value of Δt, the number of local minima and maxima increases (see Fig. 1), around which we find scale-free behavior, for exactly the same ε interval $0.6 \leq \varepsilon \leq 1.4$. The peaks in $\sigma^2(\varepsilon)$ and $v(\varepsilon)$ around $\varepsilon = 1$ and the dip of $\tau(\varepsilon)$ around $\varepsilon = 1$ offer a challenge for multi-agent based financial market models [41–47] to reproduce these empirical facts. The characterization of volatility, volume, and inter-trade times by power law relationships in the time domain supports our hypothesis that a fluctuating price time series passes through a sequence of "phase transitions" [48].

Before concluding, we may ask "what kind of phase transition" could the end of a microtrend or macrotrend correspond to, or is the end of a trend an altogether different kind of phase transition that resembles all phase transitions by displaying a regime of scale free behavior characterized by a critical exponent. It may be premature to speculate on possible analogies, so we will limit ourselves here to describe what seems to be a leading candidate. Consider a simple Ising magnet characterized by one-dimensional spins that can point North or South. Each spin interacts with some (or even with all) of its neighbors with positive interaction strength J, such that when J is positive neighboring spins lower their energy by being parallel. The entire system is bathed in a magnetic field that interacts with all the spins equally with a strength parametrized by H, such that when H is positive the field points North and when H is negative the field points South. Thus, when H is positive, the system lowers its energy by each spin pointing North. Thus, there are two competing control parameters J and H. If, e.g., the system is prepared in a state with the majority of spins pointing North yet the field H points South, the competition will be between the relative effects of J and H: the J interaction motivates the spins to point North but the H interaction motivates the spin to point South. Such a system is termed *metastable* since if each North-pointing spin suddenly flips its state to point South, the system can achieve a lower total energy. This flipping will occur in time in a fashion not unlike the trading frequency near the end of a trend: first one or two spins will randomly switch their state, then more, and suddenly in an "avalanche" the majority of spins will point South. The phase transition is termed a spinodal singularity, characterized by its own set of exponents. Why should the end of microtrends or macrotrends have a parallel with the metastable physical system? Presumably near the end of a positive trend, all the market participants watching the market begin to sense that the market is metastable and that if they do not sell soon, it could be too late to make any profit because the price will drop. First a few traders sell, pushing the market imperceptibly lower. Then additional traders, sensing this microscopic downturn, may decide that now is the time to sell and they too sell. Then an "avalanche" of selling begins, with traders all hoping to protect their profits by selling before the market drops. Thus, the set of N market participants "holding their position" are in this sense analogous to the set of N mostly North-pointing spins, bathed in a South-pointing magnetic field.

The above analogy may not be the best and it will be future challenge to find a coherently convincing explanation for why the end of a microtrend or macrotrend displays such striking parallels to a phase transition. In any case, the set of interacting spins surely is analogous to the set of interacting traders.

The end of the negative microtrend or macrotrend is the same mechanism but with everything reversed. The N Ising spins point mostly South, the magnetic field is North, and the spins flip from South to North one by one and the conclude in an avalanche corresponding to the spinodal singularity. Analogously, the N traders begin to suspect that the market is becoming metastable, so they one by one start to buy and as all the traders witness the price increasing, they jump in to buy before the price becomes too high.

In summary we have seen that each trend – microtrend and macrotrend – in a financial market starts and ends with a unique switching process, and each extremum shares properties of macroscopic cooperative behavior. We have seen that the mechanism of bubble formation and bubble bursting has no scale for time scales varying over nine orders of magnitude down to the smallest possible time scale – the scale of single transactions measured in units of 10 ms. On large time scales, histograms of price returns provide the same scale-free behavior. Thus, the formation of positive and negative trends on all scales is a fundamental principle of trading, starting on the smallest possible time scale, which leads to the non-stationary nature of financial markets as well as to crash events on large time scales. Thus, the well-known catastrophic bubbles occurring on large time scales – such as the most recent financial crisis – may not be outliers but in fact single dramatic representatives caused by the scale-free behavior of the forming of increasing and decreasing trends on time scales from the very large down to the very small.

Acknowledgements The authors thank K. Binder, S.V. Buldyrev, C. De Grandi, S. Havlin, D. Helbing, U. Krey, H.-G. Matuttis, M.G. Mazza, I. Morgenstern, W. Paul, J.J. Schneider, R.H.R. Stanley, T. Vicsek, and G.M. Viswanathan for discussions, and we also thank the German Research Foundation (DFG), the Gutenberg Academy, and the NSF for financial support.

References

1. Anderson PW (1972) Science 177:393
2. Stanley HE (1971) Introduction to phase transitions and critical phenomena. Oxford University Press, London
3. Stanley HE (1999) Rev Mod Phys 71:358
4. Stanley HE, Amaral LAN, Gabaix X, Gopikrishnan P, Plerou V, Rosenow B (1999) Physica A 301:126
5. Mantegna RN, Stanley HE (2000) Introduction to econophysics correlations and complexity in finance. Cambridge University Press, Cambridge, MA
6. Axtell RL (2001) Science 293:1818
7. Takayasu H (ed) (2006) Practical fruits of econophysics. Springer, Berlin
8. Kiyono K, Struzik ZR, Yamamoto Y (2006) Phys Rev Lett 96:068701
9. Watanabe K, Takayasu H, Takayasu M (2007) Physica A 383:120
10. Gabaix X, Gopikrishnan P, Plerou V, Stanley HE (2003) Nature 423:267

11. Preis T, Paul W, Schneider JJ (2008) Europhys Lett 82:68005
12. Lillo F, Farmer JD, Mantegna RN (2003) Nature 421:129
13. Plerou V, Gopikrishnan P, Gabaix X, Stanley HE (2002) Phys Rev E 66:027104
14. Cont R, Bouchaud JP (2000) Macroecon Dyn 4:170
15. Krawiecki A, Holyst JA, Helbing D (2002) Phys Rev Lett 89:158701
16. O'Hara M (1995) Market microstructure theory. Blackwell, Cambridge, MA
17. Vandewalle N, Ausloos M (1997) Physica A 246:454
18. Eisler Z, Kertész J (2006) Phys Rev E 73:046109
19. Mandelbrot B (1963) J Business 36:394
20. Fama EF (1963) J Business 36:420
21. Lux T (1996) Appl Finan Econ 6:463
22. Guillaume DM, Dacorogna MM, Davé RR, Müller UA, Olsen RB, Pictet OV (1997) Fin Stochastics 1:95
23. Gopikrishnan P, Meyer M, Amaral L, Stanley HE (1998) Eur J Phys B 3:139
24. Plerou V, Gopikrishnan P, Rosenow B, Amaral LAN, Stanley HE (1999) Phys Rev Lett 83:1471
25. Gopikrishnan P, Plerou V, Amaral LAN, Meyer M, Stanley HE (1999) Phys Rev E 60:5305
26. Gopikrishnan P, Plerou V, Gabaix X, Stanley HE (2000) Phys Rev E 62:4493
27. Krugman P (1996) The self-organizing economy. Blackwell, Cambridge, MA
28. Shleifer A (2000) Inefficient markets: an introduction to behavioral finance. Oxford University Press, Oxford
29. Helbing D, Farkas I, Vicsek T (2000) Nature 407:487
30. Bunde A, Schellnhuber HJ, Kropp J (eds) (2002) The science of disasters: climate disruptions, heart attacks, and market crashes. Springer, Berlin
31. Jones CM, Kaul G, Lipson ML (1994) Rev Fin Stud 7:631
32. Chan L, Fong WM (2000) J Fin Econ 57:247
33. Politi M, Scalas E (2008) Physica A 387:2025
34. Jiang ZQ, Chen W, Zhou WX (2009) Physica A 388:433
35. Dubil R (2004) An arbitrage guide to financial markets. Wiley, Chichester
36. Deutsch HP (2001) Derivate und interne modelle: modernes risk management. Schaefer-Poeschel, Stuttgart
37. Binder K (1987) Rep Prog Phys 50:783
38. Peng CK, Mietus J, Hausdorff JM, Havlin S, Stanley HE, Goldberger AL (1993) Phys Rev Lett 70:1343
39. Helbing D, Huberman BA (1998) Nature 396:738
40. Ivanov PC, Yuen A, Podobnik B, Lee Y (2004) Phys Rev E 69:056107
41. Smith E, Farmer JD, Gillemot L, Krishnamurthy S (2003) Quant Finance 3:481
42. Lux T, Marchesi M (1999) Nature 397:498
43. Preis T, Golke S, Paul W, Schneider JJ (2006) Europhys Lett 75:510
44. Preis T, Golke S, Paul W, Schneider JJ (2007) Phys Rev E 76:016108
45. Bouchaud JP, Matacz A, Potters M (2001) Phys Rev Lett 87:228701
46. Haerdle W, Kleinow T, Korostelev A, Logeay C, Platen E (2008) Quant Fin 8:81
47. Halla AD, Hautsch N (2007) J Fin Markets 10:249
AQ1 48. Preis T, Schneider JJ, Stanley HE (2009) Formation and bursting of financial bubbles. (Preprint)

AUTHOR QUERY

AQ1. Please update reference [48].